JOURNAL OF GEOPHYSICAL RESEARCH, VOL. 103, NO. B4, PAGES 7247–7263, APRIL 10, 1998

A delineation of the Nojima fault ruptured in the $M7.2$ Kobe, Japan, earthquake of 1995 using fault zone trapped waves

Yong-Gang Li and Keiiti Aki

Department of Earth Sciences, University of Southern California, Los Angeles

John E. Vidale

Department of Earth and Space Sciences, University of California, Los Angeles

Mark G. Alvarez

Department of Geophysics, Stanford University, Stanford, California

Abstract. We used four linear seismic arrays of portable seismometers at the northern Awaji Island, Japan, to record fault zone trapped waves from aftershocks of the 1995 $M7.2$ Hyogoken Nanbu (Kobe) earthquake from April to June 1996. Three arrays were deployed across the Nojima fault, which ruptured during the mainshock, while one array was deployed across the Higashiura fault, which did not break recently. We observed significant fault zone trapped waves with relatively large amplitudes and the long wave train following S waves only when both the stations and aftershocks were located close to the Nojima fault. The coda-normalized spectral amplitudes of trapped waves show a maximum peak at 4-7 Hz, which decreases rapidly with distance from the fault trace. The normalized amplitudes of trapped waves also show a decrease with hypocentral distance along the fault, giving an apparent Q of approximately ~25 at 4-7 Hz. In comparison, the array across the Higashiura fault recorded much shorter wave trains with higher frequencies after S arrivals for the same events. We simulate these trapped waves as S waves guided in a low-velocity waveguide sandwiched between high-velocity wall rocks. We find an adequate fit by using a waveguide 60 m wide at the northern site and 30-40 m wide elsewhere along the Nojima fault, a waveguide S velocity of 1.5-1.7 km/s, and a Q value of 25. For the Higashiura fault, the S velocity is 2.5 km/s, and the Q value is 80. The locations of aftershocks for which we observed fault zone trapped waves show that the Nojima waveguide is 9 km long and dips southeastward at 80^{o}-85^{o} to a depth of ~16 km. It extends 6 km farther southwestward along the Asano fault, though there are no obvious surface breaks along it. However, the waveguide is disconnected from the Suma fault on the main island, which was also ruptured during the Kobe earthquake, possibly because of the existence of an offset between the Nojima fault and the Suma fault.

1. Introduction

The destructive $M7.2$ Kobe (Hyogoken Nanbu) earthquake of January 17, 1995, was located 20 km southwest of downtown Kobe, Japan (Figure 1), and has a strike-slip mechanism [*Kikuchi*, 1995] that accommodated east-west shortening of the Eurasian plate, which is colliding with the North American plate [*Huzita*, 1980; *Oike*, 1992]. This event was preceded by a sequence of intraplate earthquakes with similar mechanisms in central western Japan, including the $M8$ Nobi earthquake of 1891, the $M7.3$ Tango earthquake of 1927, the $M7.2$ Tottori earthquake of 1943, and the $M7.1$ Fukui earthquake of 1948 [*Kanamori*, 1973; *Usami*, 1987].

The Kobe area has a complex geological structure [*Huzita and Kazama*, 1980]. Numerous active faults are distributed along the inner zone of central to southwest intraplate Japan [*Research Group for Active Faults in Japan*, 1991]. Most of the slips on these intraplate active faults are 0.1-1.0 mm/yr and generate shallow, destructive earthquakes with repeat times of ~1000 years [*Okada and Ikeda*, 1991]. However, recent paleoseismological studies [*Awata et al.*, 1996; *Sangawa et al.*, 1996] around the rupture zone of the Kobe earthquake suggest that the interval between the two most recent events on this fault system is ~400 years. The right-lateral Rokko fault system that runs from Awaji Island to Kobe had been mapped before the earthquake. Because of the numerous active Quaternary faults and historic damaging earthquakes, this district was designated as a potential seismic hazard area [e.g., *Oike*, 1992]. However, reliable earthquake prediction is difficult because intraplate earthquakes can occur on any one of the faults, each having a repeat time of hundreds to thousands of years [*Shimazaki and Nakata*, 1980; *Kanamori*, 1995].

The Kobe earthquake produced a 9-km-long surface break with the maximum right-lateral slip of 1.9 m along the Nojima fault on Awaji Island southwest of the mainshock epicenter [*Nakata and Yomogida*, 1995; *Yomogida and Nakata*, 1995]. No significant surface ruptures were found on the main island,

Paper number 98JB00166.
0148-0227/98/98JB-00166$09.00

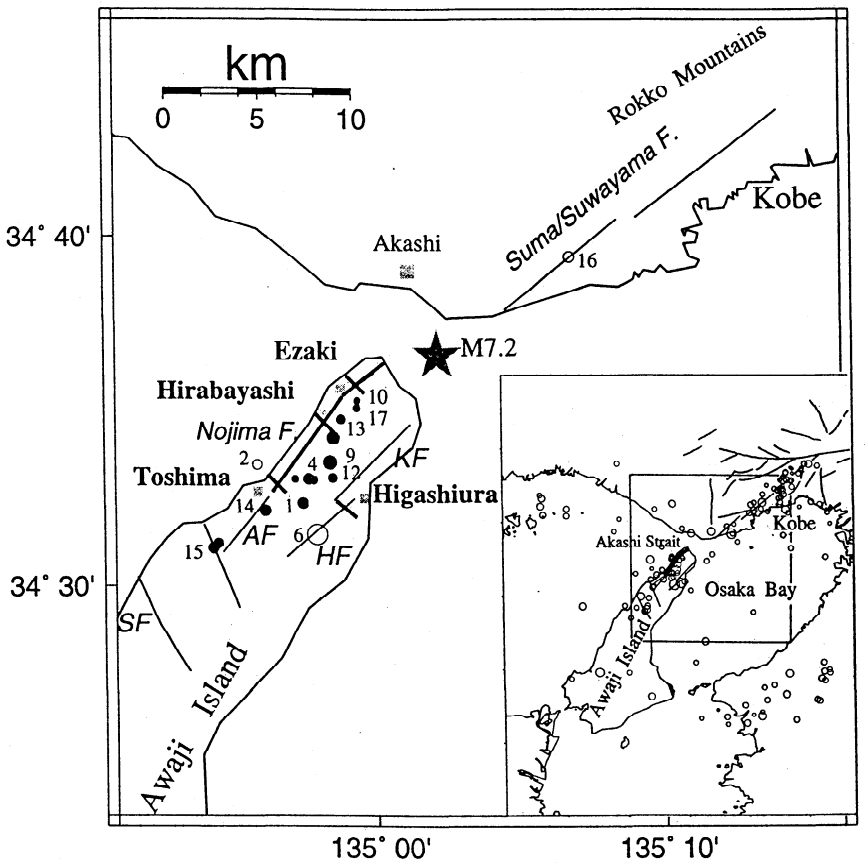

Figure 1. Map showing locations of four linear seismic arrays (solid bars) deployed on Awaji Island, Japan. The arrays were named after nearby towns (shaded squares). Open circles are epicenters of aftershocks with magnitudes of $M1.0$ to $M3.0$ occurring in the working area (inset) during the experiment. Locations of these events are from the automatic hypocenter location system at Disaster Prevention Research Institute, Kyoto University. Solid circles denote the aftershocks for which we observed trapped waves. The events for which waveforms are shown in this paper are labeled by a number. The star denotes the mainshock epicenter. Thin lines are fault traces. The Nojima fault is denoted by thick lines. AF, Asano fault; HF, Higashiura fault; KF, Kusumoto fault; SF, Shichiku fault.

Table 1. Locations, Times, and Magnitudes of Aftershocks Exciting Fault Zone Trapped Waves

Event	Julian Day	Date 1996	Origin Time, UT	Latitude, N	Longitude, E	Depth, km	Magnitude
1	119	April 28	0942:06.4	34°32.31'	134°57.59'	16.2	1.9
3	121	April 30	1424:56.3	34°31.22'	134°54.52'	12.0	1.7
4	123	May 3	2050:12.7	34°33.05'	134°57.86'	16.0	1.6
5	129	May 9	2333:26.7	34°34.25'	134°58.57'	14.8	2.1
7	132	May 11	0608:17.3	34°33.07'	134°57.68'	13.1	1.9
8	139	May 18	0045:57.1	34°35.10'	134°59.44'	10.7	1.6
9	145	May 25	2032:58.2	34°33.55'	134°58.45'	11.5	2.3
10	146	May 26	1534:37.1	34°35,30'	134°59.40'	8.5	1.1
11	150	May 29	1451:00.0	34°33.07'	134°57.21'	15.3	1.2
12	151	May 31	2117:42.5	34°33.10'	134°58.53'	14.3	1.5
13	152	May 31	0334:23.6	34°34.78'	134°58.84'	11.5	1.6
14	157	June 5	0024:50.6	34°32.16'	134°56.17'	14.2	1.8
15	158	June 6	0818:36.1	34°31.10'	134°54.36'	12.9	1.9
17	159	June 8	2133:54.2	34°35.10'	134°59.38'	10.7	1.3

Locations and times were based on the catalog of the automatic hypocenter location system at Disaster Prevention Research Institute, Kyoto University; some events were located using the data from portable arrays in this experiment.

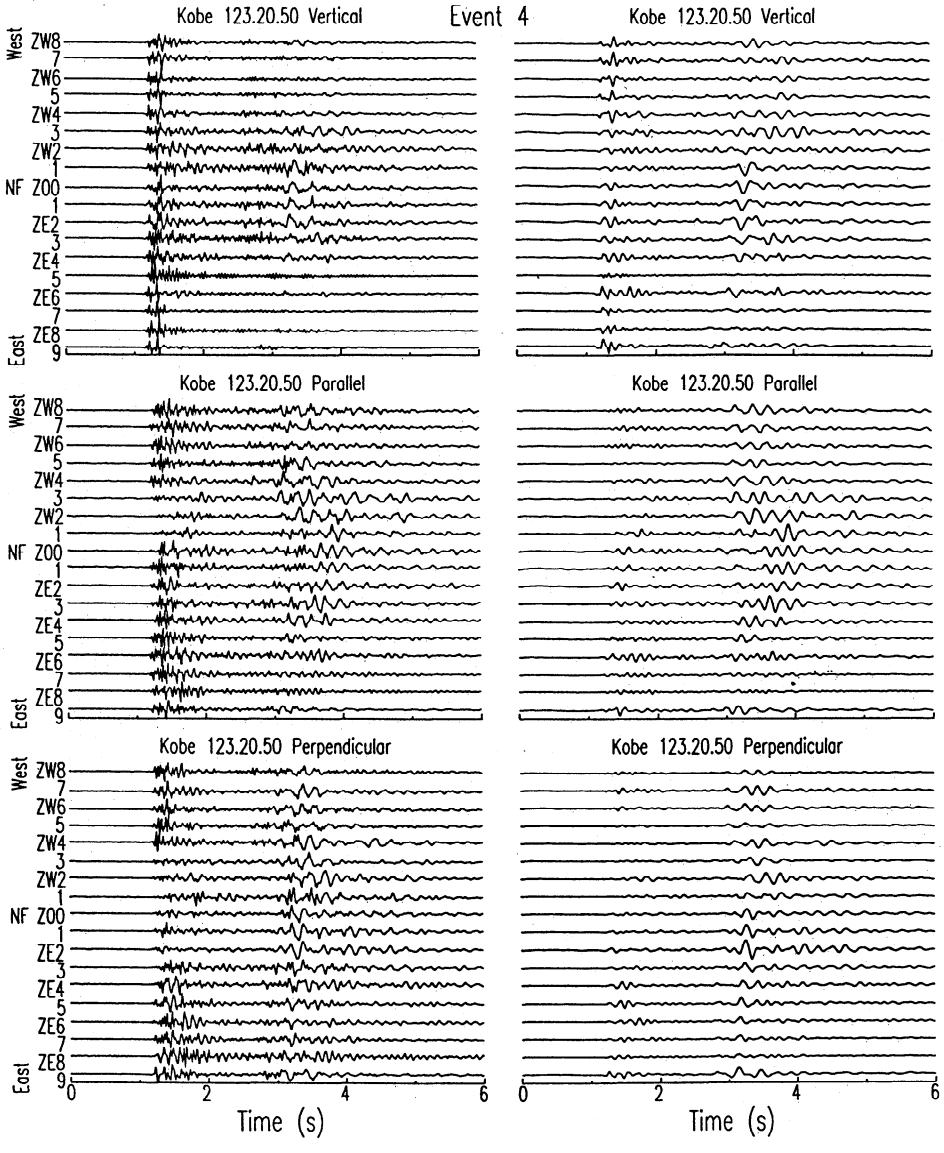

Figure 2a. Vertical, fault zone-parallel, and fault zone-perpendicular components of seismograms recorded at the Ezaki array for event 4 on the Nojima fault. The date (Julian day, hour, and minute) is given for each seismogram. Each trace is plotted using a peak-to-peak amplitude scale and labeled by the station name. NF denotes the corresponding location of the Nojima fault trace. Low-pass-filtered (< 6 Hz) seismograms are plotted at right using a common scale for all traces. Fault zone trapped waves with relatively large amplitudes and long periods are shown between 3 and 5 s at stations close to the fault trace.

probably because of the thick sedimentary strata overlying the bedrock around the Osaka Bay. Inversions of near-source ground motions, teleseismic body waveforms and geodetic displacements of the Kobe earthquake [e.g., *Kikuchi*, 1995; *Pitarka et al.*, 1995; *Wald*, 1995, 1996; *Ide et al.*, 1996; *Yoshida et al.*, 1996] showed a complex source process with multiple subevents triggered on segmented slip planes, in accordance with the distribution of the faults in the region, including the Nojima fault on Awaji Island and the Suma-Suwayama faults on the main island. *Wald* [1996] presented a slip model using two-planar rupture planes; the southwestern plane (Nojima) is 20 km long and dips 80° to southeast, whereas the northeastern plane (Suma) is 40 km long and dips 85° to northwest. The mainshock nucleated on the southwest end of the Suma fault with bilateral faulting. Between the two rupture planes, there is an offset near the epicenter. The coseismic displacements derived from continuous Global Positioning System (GPS) and leveling also indicated multiple rupture segments in the aftershock areas [*Hashimoto*, 1995]. A discontinuity in the displacement field southeast of Akashi Strait suggests that the fault offset there. However, *Nakamura and Ando* [1995] point out that the fault geometry at surface does not correspond to the distribution of aftershocks at the Awaji area and that fault surface traces may not connect directly with the underground fault geometry estimated by aftershock distribution.

In this study, we use fault zone trapped waves to delineate the fine structure of the faults ruptured in the Kobe earthquake. In the past decade, such waves have been observed at many active faults in California and used as probes of the state of the fault zone at the seismological depth [e.g. *Li et al.*, 1990; *Li and Leary*, 1990; *Leary et al.*, 1991; *Li et al.*, 1994a, b; *Hough et al.*, 1994; *Malin and Lou*, 1995; *Jongmans and Malin*, 1995; *Li et al.*, 1997a, b]. These waves can be excited either

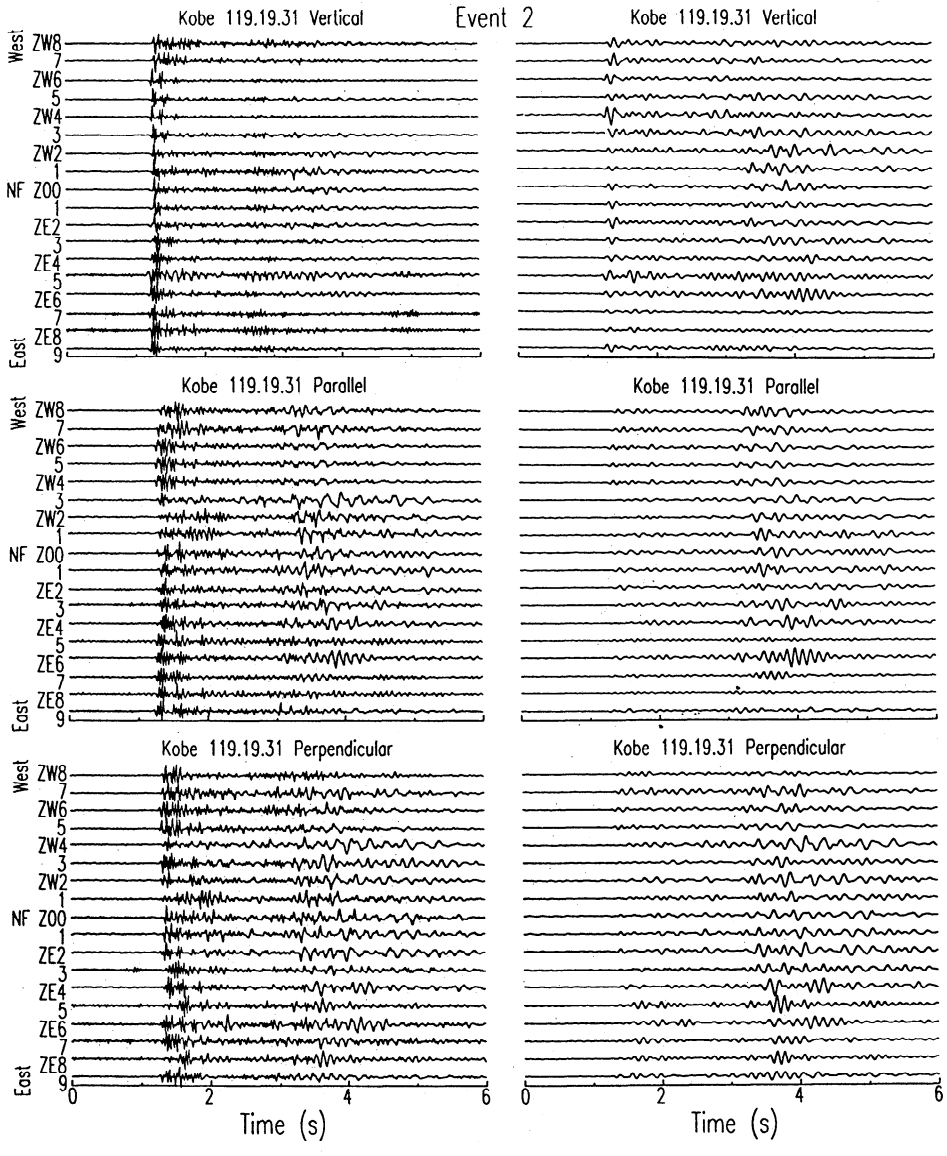

Figure 2b. Three-component raw and low-pass-filtered (< 6 Hz) seismograms recorded at the Ezaki array for event 2. The event occurred too far away from the Nojima fault to excite significant trapped waves.

by earthquakes or explosions, as long as the sources are located within the fault zone. Since the waves arise from coherent multiple reflections at the boundaries between the low-velocity fault zone and the high-velocity surrounding rock, their amplitudes and frequencies are strongly dependent on the fault geometry and physical properties. Thus observation and modeling of fault zone trapped waves may reveal the fine structure and continuity of the fault zone at depth.

2. Data Acquisition

From mid-April to mid-June 1996, we deployed 55 three-component portable seismometers from Incorporated Research Institutions for Seismology (*IRIS*) on Awaji Island in four 220-300-m-long linear arrays; three across the Nojima fault, which ruptured in the Kobe earthquake and one across the Higashiura fault, which did not break recently (Figure 1). These two faults are ~5 km apart along the northwest and southeast coasts of the northern Awaji Island.

The three arrays across the Nojima fault named after nearby local towns, Ezaki, Hirabayashi, and Toshima, were located about ~3, 6, and 9 km southwest of the mainshock epicenter. At Ezaki, the Nojima fault has an interconnected pattern of stepping, en echelon cracks and fissures, tilted and rotated blocks, and small-scale pull-apart and pop-up structures with 0.9-1.3 m total horizontal displacement and 0.5 m total vertical offset [*Hamilton et al.*, 1995]. A steel power-line tower at this site fell down in the Kobe earthquake. A thin sedimentary cover is on the granite bedrock northwest of the fault. The array ran along a lane sloping gently downhill toward the coast. At Hirabayashi, the Nojima fault has the maximum right-lateral surface slip of 1.9 m and a vertical scarp of 1.2 m caused by the Kobe earthquake. The fault is sandwiched between granite outcrops to the southeast and a sedimentary coastal basin to the northwest. The site has irregular topography of terraces with 3- to 5-m steps for each. At Toshima, the Nojima fault was dislocated 1.2 m horizontally and 0.4 m vertically. The site is flat, but drilling at this site showed a sedimentary layer overlying bedrock on both sides of the fault (*Ikeda, University of Southern California*, oral communication, 1997). The fourth array across the northern Higashiura fault was located in a rice field where a trench was dug across the Higashiura fault trace by the

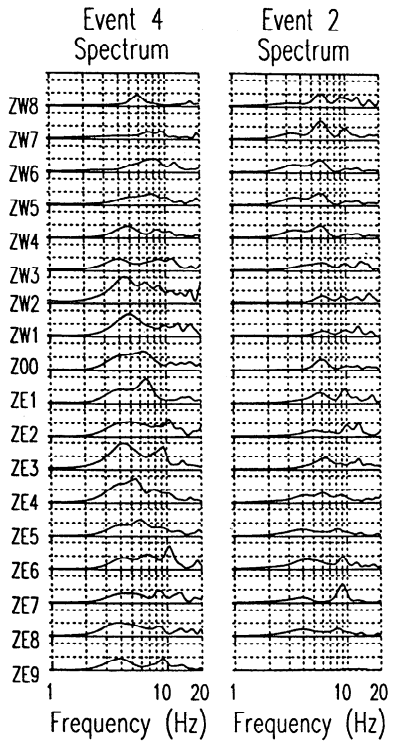

Figure 2c. The coda-normalized amplitude spectra of fault zone-parallel component seismograms calculated in a 2-s time window starting from *S* arrivals; the time window for coda waves has the same length starting from 15 s after the event origin time. The spectra are plotted using a fixed amplitude scale of 50. The peak amplitudes at 4-6 Hz appear at stations close to the fault trace.

Geological Survey of Japan after the earthquake. The Higashiura array was ~8 km southwest of the mainshock epicenter.

The Ezaki and Toshima arrays had 18 stations each, whereas the Higashiura and Hirabayashi arrays had 13 stations each, all centered on the fault trace. The station spacing across the Nojima fault is 10 m for the five central stations and 20 m for the others. The spacing of the Higashiura array is 10 m for the three central stations and 20 m for the others. The sensors (Mark product L22) were buried to avoid wind noises, with the three components aligned vertical and parallel and perpendicular to the fault trace. All stations were synchronized through Global Positioning System (GPS). The GPS also provided the longitude and latitude of the stations. The Ezaki array centered at E134°59'10.75", N34°35'59.32", the Hirabayashi array centered at E134°58'01.37", N34°34'56.21", the Toshima array centered at E134°56'16.73", N34°32'59.34", and the Higashiura array centered at E134°58'49.31", N34°32'11.02". The Ezaki and Toshima arrays were operated for ~2 months, whereas the Higashiura and Hirabayashi arrays for ~1 month each. The seismometers recorded continuously at a rate of 100 samples per second on an internal 500-Mbyte hard disk. We transferred the data from one seismic array to a Sun computer every other day in the field.

3. Results

About 80 aftershocks with magnitudes of $M1.0$-$M3.2$ occurred in the Awaji-Kobe area during the deployment period (Figure 1). Locations of these events are based on the catalog of local seismicity from the automatic hypocenter location system at Disaster Prevention Research Institute, Kyoto University. The data recorded for these events were processed as follows: (1) sorting the events based on the catalog of local seismicity, (2) selecting well-recorded events that occurred within a distance of 30 km from the arrays, (3) searching for events with long-period, large-amplitude wave trains following *S* waves, (4) calculating coda-normalized amplitude spectra of wave trains in a selected time window starting from the arrival of *S* waves, (5) modeling the observed trapped waves to characterize the fault zone, and (6) plotting hypocenters of events with and without fault zone trapped waves to delineate the fault zone. Table 1 lists 14 events for which we observed fault zone trapped waves.

Figure 2a shows the three-component raw and low-pass-filtered seismograms recorded at the Ezaki array from a $M1.6$ aftershock (event 4 in Figure 1 and Table 1) occurring northeast of Toshima town. We observed fault zone trapped waves with relatively large amplitudes, low frequencies, and long duration following *S* arrivals at stations located close to the fault trace. However, such wave trains did not appear at the other stations that were located farther from the fault trace, although they all recorded the high-frequency body waves. The trapped waves were most obvious in the fault zone-parallel component for this event.

To analyze the trapped waves, we calculated the amplitude spectra for a 2-s time window (200 samples for Fourier transformation) starting from the *S* arrivals, using a Hanning window with a 20-ms taper to include the trapped waves. In order to eliminate source, site, and instrument effects on the spectral amplitudes of trapped waves, we used the coda normalization method of *Aki* [1969], which we have also used for studying fault zone guided waves at the Landers, California, faults [*Li et al.*, 1994a]. We take the beginning of the coda window at 15 s measured from the earthquake origin time, allowing source-receiver pairs within ~25 km for normalization. The coda-normalized amplitude spectra for event 4 (Figure 2c) show a maximum at 4-6 Hz for stations located close to the fault trace between ZW2 and ZE4. The distance between ZW2 and ZE4 is 80 m. The amplitudes at 4-6 Hz become less prominent with increasing distance from the fault. We think that event 4 may have occurred on the Nojima fault and excited trapped waves of such characteristics within the low-velocity zone along the Nojima fault. To account for the 16.2-km focal depth and 2.1-km offset of this event from the fault trace, we estimate that the Nojima fault dips southeastward at ~83°.

For comparison, Figure 2b shows seismograms recorded at the Ezaki array from a $M1.6$ aftershock (event 2 in Figure 1) occurring on April 28 about 2 km west of the Nojima fault. The location of this event is at E135°55.91', N34°33.49' and a depth of 14.4 km. No significant fault zone trapped waves were observable, even though event 2 was the same magnitude and at the same distance from the array as event 4 and generated similar waves at higher frequencies. The corresponding coda-normalized amplitude spectra of seismograms show no peaks at frequencies below 6 Hz for stations located within the fault zone (Figure 2c). The larger amplitudes at 6-7 Hz were registered at stations located west of the fault because this event occurred on the same side. We interpret that event 2 occurred too far away from the Nojima fault to generate fault zone trapped modes.

Figure 3 shows seismograms recorded at the Ezaki array for events 9 and 12, which generated significant fault zone trapped waves. The coda-normalized amplitude spectra of trapped waves show a maximum peak at 4-6 Hz for stations close to the Nojima fault trace, which decreases rapidly with the distance from the fault trace. The epicenters of these two aftershocks were located ~2-3 km southeast of the Nojima fault trace, again indicating a fault dip to the southeast.

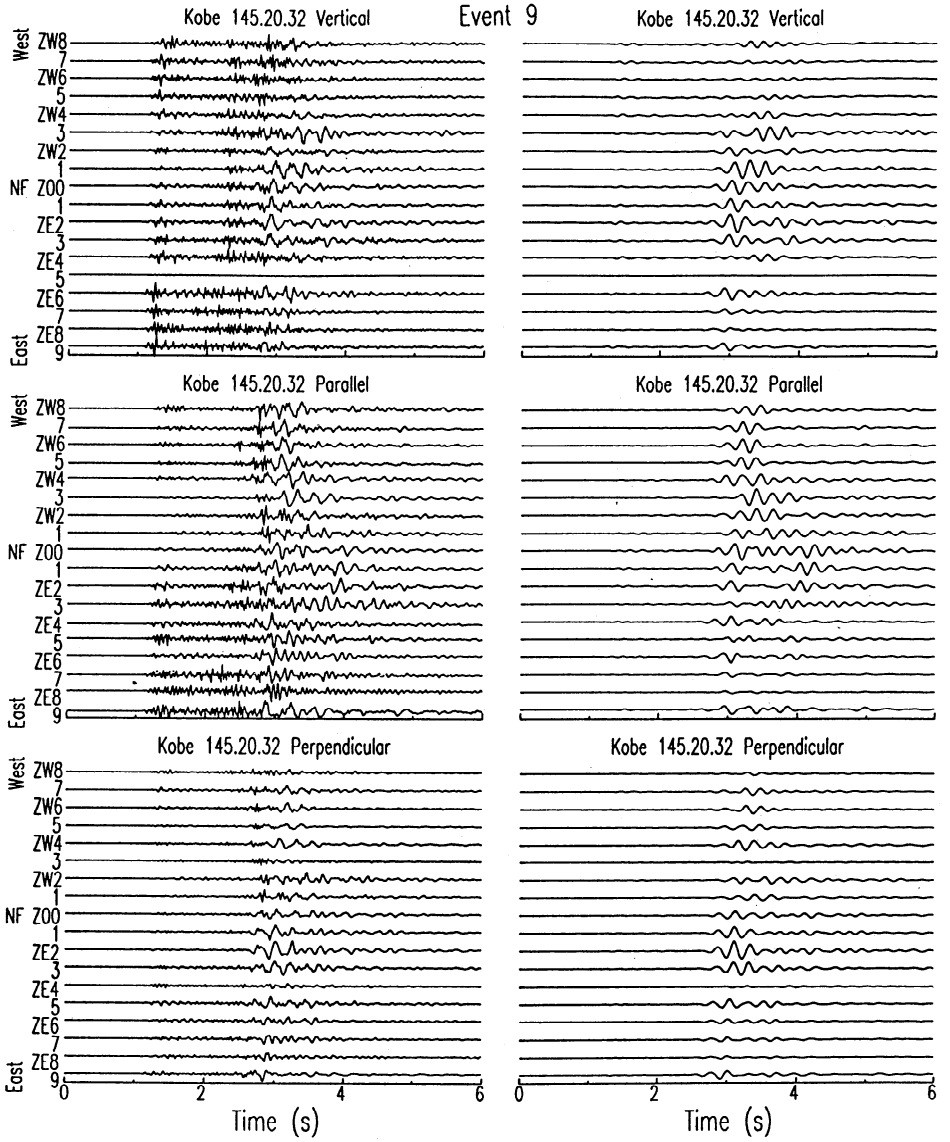

Figure 3a. Three-component raw and low-pass-filtered (< 6 Hz) seismograms at the Ezaki array for event 9 occurring on the Nojima fault. Fault zone trapped waves are shown between 3 and 5 s at stations close to the fault trace.

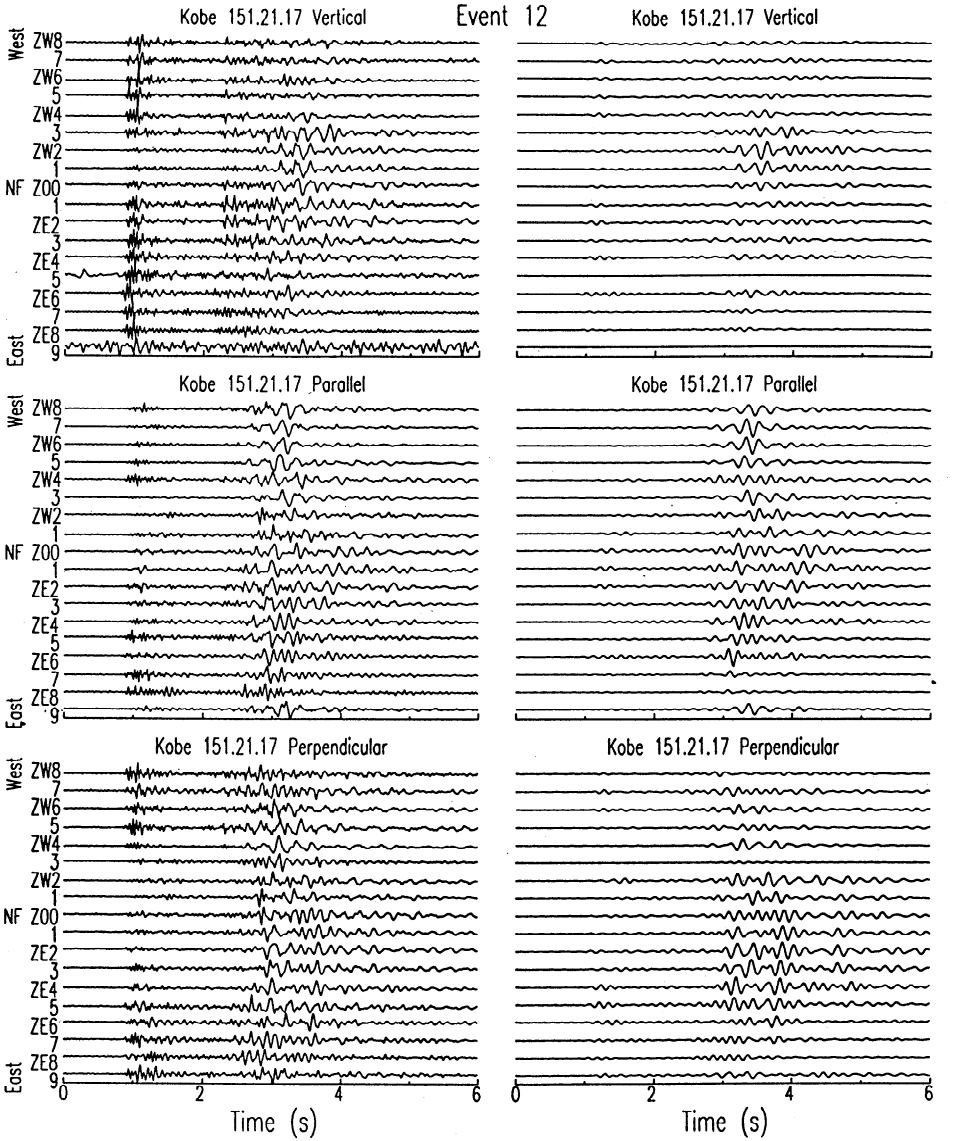

Figure 3b. Same as Figure 3a, except for event 12 on the Nojima fault.

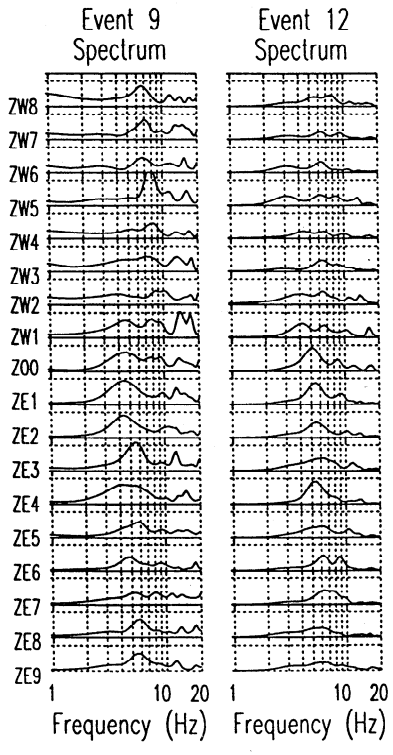

Figure 3c. Normalized amplitude spectra plotted using a fixed amplitude scale of 65. Other notations are the same as in Figure 2.

Significant fault zone trapped waves were also generated by the aftershocks on the Asano fault, which is an active strand southwest of the Nojima fault, but no obvious surface breaks were found along it after the Kobe earthquake (Figure 1). Figure 4a shows seismograms recorded at the Ezaki array for event 15 occurring at the south end of the Asano fault. The normalized amplitude spectra of trapped waves show a maximum peak at 5-7 Hz at stations close to the Nojima fault trace, which rapidly decays at stations farther away from the fault trace (Figure 4c). The trapped waves from event 15 arrived at the Ezaki array with the greater time delay after S waves and smaller amplitudes than those from events 4, 9, and 12 because it had the longer travel distance. This observation suggests that the low-velocity waveguide on the Nojima fault may extend southwestward along the Asano fault.

On the other hand, we did not observe fault zone trapped waves at arrays deployed at the Nojima fault for aftershocks on the main island, including those events occurring on the Suma and Suwayama faults, which had been ruptured in the Kobe earthquake. As an example, Figure 4b shows seismograms recorded at the Ezaki array for a M1.7 aftershock (event 16 in Figure 1) occurring on June 7 at the Suma fault. The location of this event is at E135°06.75', N34°39.41', about 13 km away from Ezaki, and a depth of 11.4 km. No trapped waves were recorded for this event; all stations registered similar high-frequency waves. The normalized amplitude spectra of seismograms show no peaks at frequencies < 8 Hz at all stations (Figure 4c). We interpret that an offset between the Nojima fault and Suma fault may disrupt the passage of trapped waves even if such trapped waves were excited within the Suma fault. *Li and Vidale* [1996] have demonstrated that a fault offset of more than several fault widths can disrupt the waveguide. At Landers, California, for example, we found that a step-over between the Johnson Valley fault and Homestead Valley fault disrupted the fault zone guide waves propagating from the Landers northern rupture segment to the southern segment and vice versa [*Li et al.*, 1994a, b].

Figure 5a shows fault zone trapped waves recorded at the Ezaki array from events 10, 17, 13, 9, 1, and 14, which occurred on the Nojima and Asano faults in a hypocentral distance range of 8-16 km. We notice that the separation between the S and trapped wave arrivals increases with the distance, as expected for trapped waves traveling along the slower fault zone waveguide. This observation confirms the continuity of the waveguide on the Nojima and Asano faults.

To study attenuation of trapped waves along the Nojima and Asano faults, we plot normalized spectral amplitudes at 4-7 Hz for eight aftershocks occurring on the faults as a function of hypocentral distance from the Ezaki array in Figure 5b. The amplitudes, although showing scatter, decrease systematically with hypocentral distance r. Assuming a waveguide S velocity of 1.6 km/s and an amplitude decay proportional to $r^{1/2}$, we obtained an apparent Q of ~25 at 4-7 Hz for the waveguide on the Nojima and Asano faults.

Next, we present the data recorded at the Higashiura array for event 4 (Figure 6a). The wave trains following S waves recorded at the Higashiura array are much shorter than at the Ezaki array for this event (refer to Figure 2a). The normalized amplitude spectra of these waves (Figure 6c) show higher frequencies (8-10 Hz) at the Higashiura array than at the Ezaki array (refer to Figure 2c). We interpret the Higashiura fault to have a velocity higher than in the Nojima fault, perhaps because it was not broken in the Kobe earthquake. However, it is still slower than the surrounding rock, and thus has some trapping efficiency. Figure 6b shows seismograms recorded at the Higashiura array for a M3.2 aftershock (event 6 in Figure 1) with the epicenter right on the surface trace of the Higashiura fault. This event occurred on May 11 at E135°06.75', N34°39.41' and a depth of 11.4 km. All stations recorded the similar waveforms but not trapped waves. On the basis of these observations, we suggest that the Higashiura fault may dip northwestward and intersect the Nojima fault at a depth above the 16.2-km focal depth of event 4, so that some trapped energy was partitioned from the Nojima fault into the Higashiura fault. However, event 6 occurred neither on the Higashiura fault nor on the Nojima fault.

We then present the data recorded at two other arrays across the Nojima fault at Hirabayashi and Toshima. We found that fault zone trapped waves were affected by the near-surface geological complexity at these two sites. Figure 7 shows seismograms recorded at the Hirabayashi array for events 12 and 14 occurring on the Nojima and Asano faults. Strong surface waves at low frequencies were recorded at stations located on the west side of the fault because of a thick sedimentary basin on this side. However, the normalized amplitude spectra show a maximum peak at 5-7 Hz at stations close to the fault trace between BW1 and BE2, which were apart 30 m. We notice that the trapped waves at Hirabayashi show higher frequencies than at the Ezaki array for the same events, suggesting that the waveguide is narrower at Hirabayashi than at Ezaki.

Figure 8 illustrates seismograms recorded at the Toshima array for events 12 and 14. Fault zone trapped waves were not shown clearly because of a thick sedimentary layer overlying the bedrock at this site. We have shown that overlying sediments with a thickness of more than a couple of fault zone widths can obscure a waveguide in numerical investigation of trapping efficiency for a low-velocity fault zone waveguide [*Li and Vidale*, 1996]. However, the recent rupture during the Kobe earthquake reached the surface at the Toshima site and thus could cause a small velocity contrast even in the overlying sediments. Indeed, the coda-normalized spectra show a maximum peak at 5-7 Hz at stations close to the fault between TW1 and TE4, which were apart 50 m.

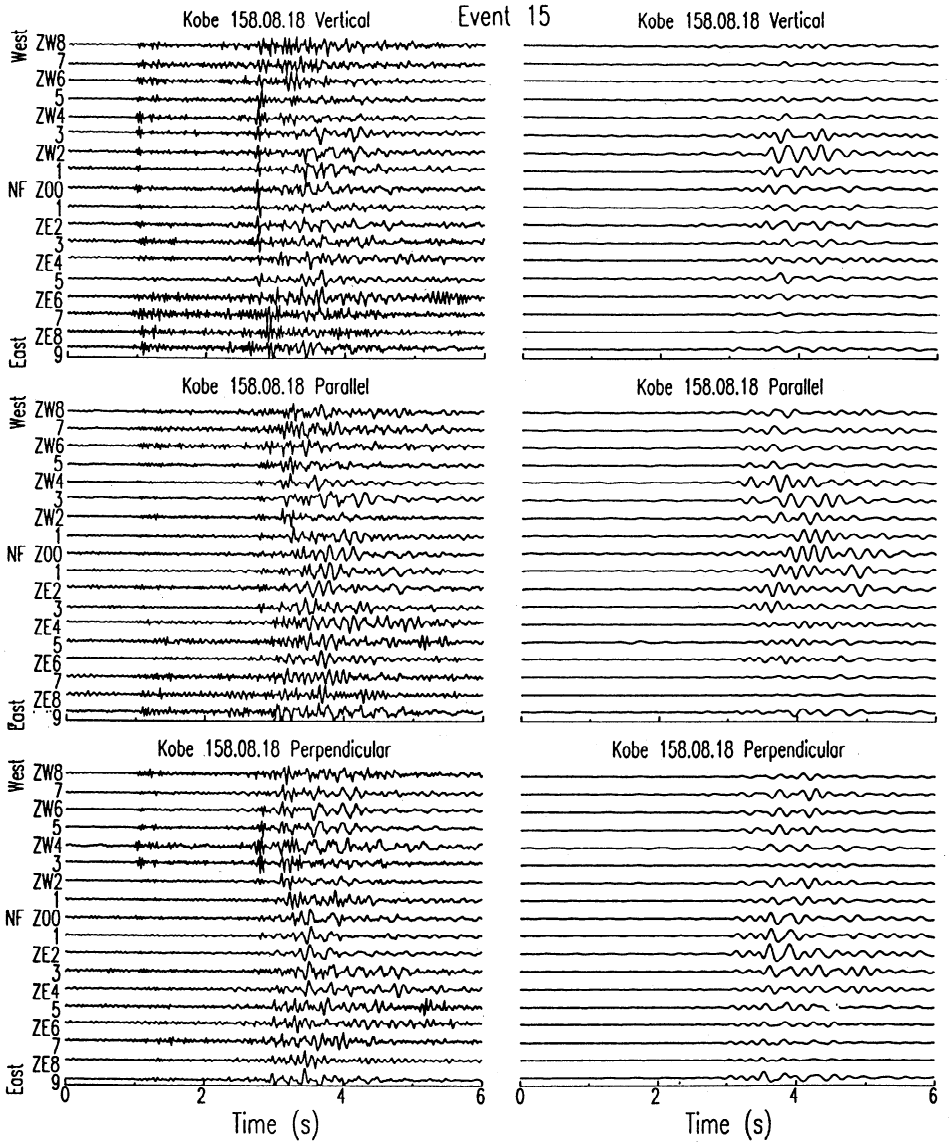

Figure 4a. Three-component raw and low-pass-filtered (< 6 Hz) seismograms at the Ezaki array for event 15 on the Asano fault. Fault zone trapped waves are shown between 3 and 6 s at stations close to the fault trace.

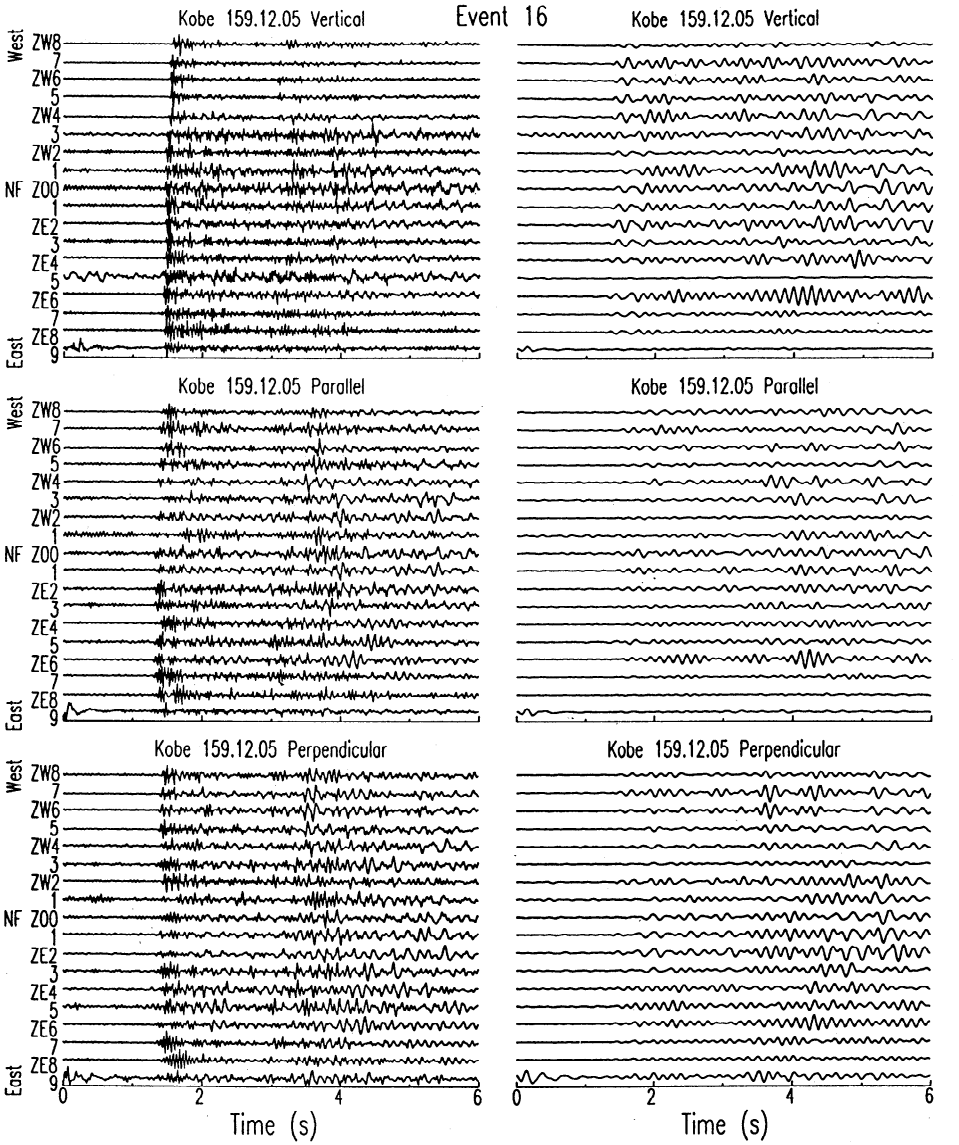

Figure 4b. Same as Figure 4a, except for event 16 on the Suma fault. No trapped waves were observed for this event.

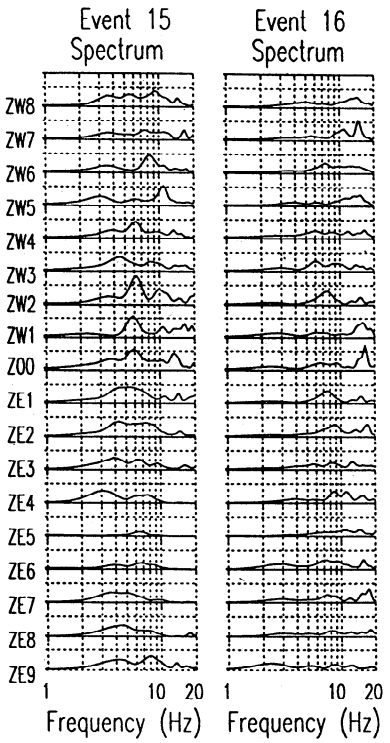

Figure 4c. Normalized spectra plotted using a fixed amplitude scale of 35. Other notations are the same as in Figure 2.

4. Distribution of Earthquakes With and Without Trapped Waves

Figure 9a shows epicenters of aftershocks occurring in the study area and period, including 14 events (solid circles) showing fault zone trapped waves. The epicenters of these 14 events distribute in a 15-km-long zone parallel to the surface traces of the Nojima and Asano faults. This zone inferred to be a low-velocity waveguide in the northern Awaji Island is longer than the total 9 km of surface breaks along the Nojima fault produced by the Kobe earthquake [*Nakata and Yomogida*, 1995; *Yomogida and Nakata*, 1995] but shorter than the ruptured length seismically estimated by *Wald* [1996]. On the other hand, the events showing no trapped waves are located elsewhere.

Because we did not observe trapped waves at arrays deployed across the Nojima fault for those events occurring on the Suma and Suwayama faults, we interpreted that the waveguide on Awaji Island is disconnected from the Suma fault on the main island, possibly due to a fault offset between the Nojima fault and Suma fault.

Figure 9b shows a vertical cross-sectional view of Nojima and Higashiura faults together with locations of the aftershocks in the studied area. Aftershocks occurring on the main island are not plotted because we did not observe trapped waves for those events. Locations of the events (solid circles) with trapped waves delineate a 16-km-deep zone between the Nojima and Higashiura surface traces. Since significant fault zone trapped waves were observed only at arrays across the Nojima surface trace, we connect this zone to the Nojima fault trace (dashed line in Figure 9b). The inferred fault plane waveguide dips to the southeast at 80°-85°, which is consistent with the borehole measurements at the Nojima fault [*Ito*, 1996]. However, the hypocenter locations of these aftershocks show a broader zone than the waveguide width obtained by modeling as shown in section 5, possibly because of small location errors for these events or three-dimensional undulations of the rupture plane.

5. Simulations of Fault Zone Trapped Waves

A quantitative estimation of fault zone width, velocity, and Q may be obtained by synthesis of waves of Love type, using a simple model of an elastic layer with relatively low velocity and Q sandwiched between two elastic half-spaces with relatively high velocity and Q. We used the phase shift method of *Li and Leary* [1990] and the formulation for the Love wave part of the Green's function given by *Aki and Richards* [1980] to compute synthetic trapped waves, as has been used for similar observations at the San Andreas fault near Parkfield [*Li et al.*, 1990; *Li et al.*, 1997a] and at Landers, California [*Li et al.*, 1994a].

Figure 10 illustrates the trapping efficiency of a waveguide with different model parameters. Figure 10a shows synthetic trapped waves and amplitude spectra for a waveguide with Q value of 100 and widths of 70, 50, and 30 m. The waveguide S velocity is assumed to be 2.0 km/s. The wall rock S velocity is assumed to be 3.0 km/s, and the Q value is assumed to be 100. A 16-element linear array with the receiver spacing of 20 m is across the waveguide. The source is located within the waveguide. The distance between the source and array is 15 km. The wider waveguide produces trapped waves with lower frequencies and longer wave trains. Figure 10b shows synthetic trapped waves and amplitude spectra for a waveguide with a Q value of 25. Other parameters are the same as in Figure 10a. The lower Q waveguide produces trapped waves with smaller amplitudes and lower frequencies. When the waveguide width is 30 m and Q = 25, the waveguide shows only a weak trapping efficiency due to the high attenuation.

Figures 10c shows synthetic trapped waves and amplitude spectra for a waveguide with Q = 25 and S velocities of 1.5, 2.0, and 2.5 km/s. The distance between the source and array is 10 km. The shorter travel distance causes shorter wave trains as compared to those in Figure 10b. However, the slower waveguide produces the longer dispersive wave trains of trapped waves. When the waveguide has a value of Q 25 and S velocity of 2.5 km/s, the waveguide has a very weak trapping efficiency and produces very short wave trains because of high attenuation and small velocity contrast between the waveguide and wall rock. Figure 10d shows that when the Q value is as low as 10, it can disrupt the trapping efficiency of a waveguide because of the serious attenuation. On the other hand, trapped waves are not affected obviously when the Q value is larger than 100.

To find waveguide parameters that best fit the observed trapped waves, we tested a range of model parameters with waveguide width varying between 20 and 100 m, waveguide S velocity between 1.0 and 2.5 km/s, and Q value between 10 and 100 in a forward modeling procedure. When the waveguide width varies 10 m, or S velocity varies 0.1 km/s, or Q value varies 10, the amplitudes and dispersion of trapped waves change observably. Figure 11 shows four examples of synthetic trapped waves and the data recorded at the Ezaki, Higashiura, Hirabayashi, and Toshima arrays. In these examples, we used model parameters listed in Table 2; the Nojima waveguide width is 60 m at Ezaki, 30 m at Hirabayashi, and 40 m at Toshima. The waveguide S velocity is 1.5-1.7 km/s, and Q = 25. The Higashiura waveguide is 35 m wide, where the S velocity is 2.5 km/s and Q = 80. The wall rock S velocity is 3.0-3.2 km/s, and Q = 100.

These parameters are not uniquely constrained because there is a trade-off among the parameters, and the method used here is simply for a uniform waveguide. Moreover, the amplitude and frequency contents of trapped waves in the calculated two-

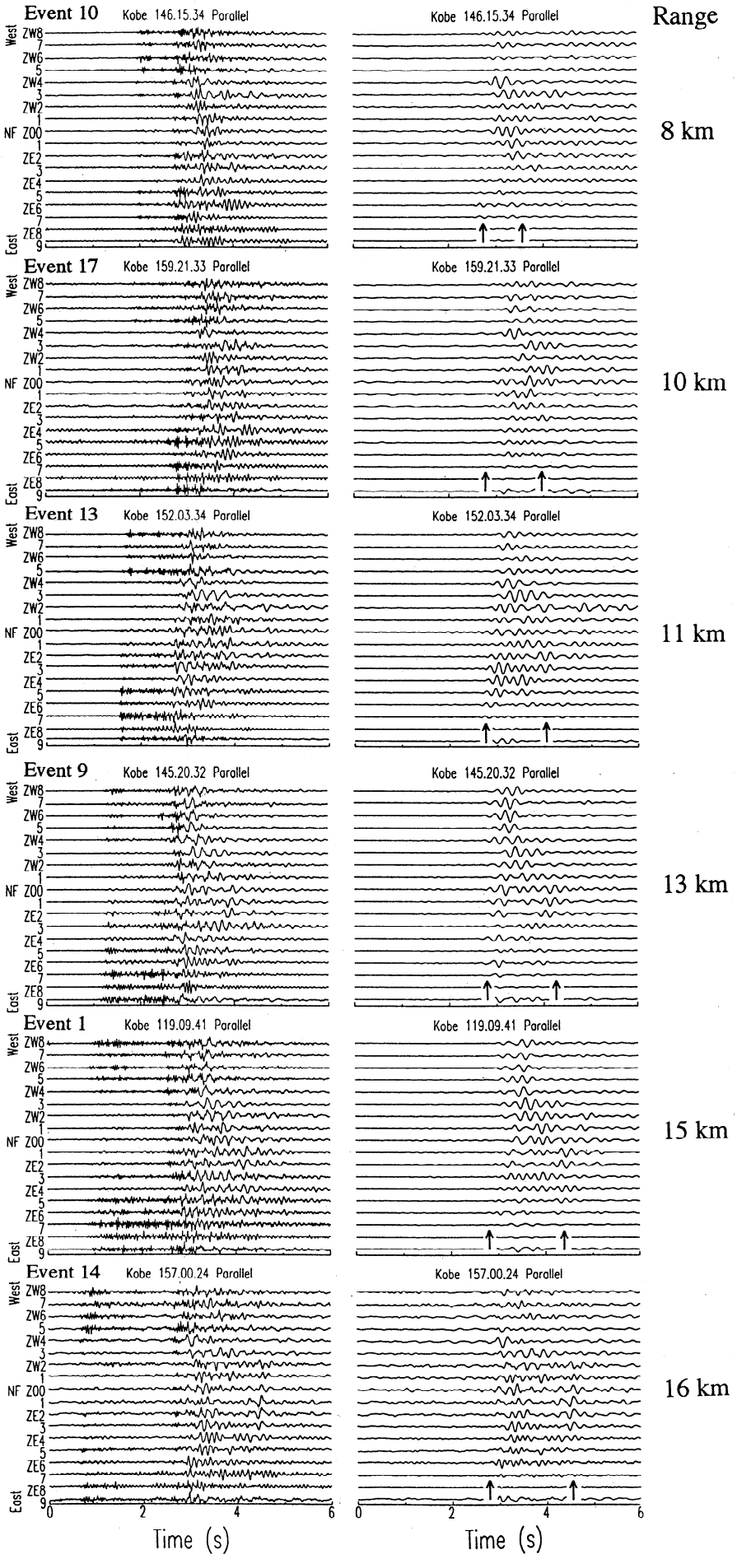
Event 10
Kobe 146.15.34 Parallel
Kobe 146.15.34 Parallel
Range
8 km
Event 17
Kobe 159.21.33 Parallel
Kobe 159.21.33 Parallel
10 km
Event 13
Kobe 152.03.34 Parallel
Kobe 152.03.34 Parallel
11 km
Event 9
Kobe 145.20.32 Parallel
Kobe 145.20.32 Parallel
13 km
Event 1
Kobe 119.09.41 Parallel
Kobe 119.09.41 Parallel
15 km
Event 14
Kobe 157.00.24 Parallel
Kobe 157.00.24 Parallel
16 km
West
East
NF
ZW8
ZW6
ZW4
ZW2
Z00
ZE2
ZE4
ZE6
ZE8
0
2
4
6
Time (s)
Time (s)

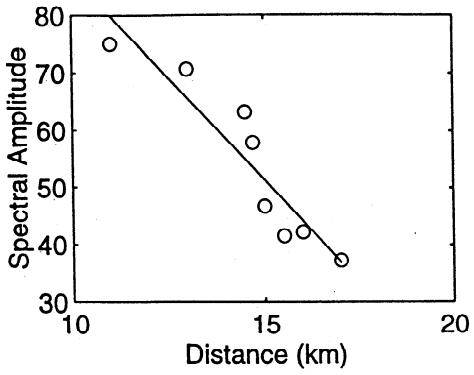

Figure 5b. The normalized peak spectral amplitudes at stations close to the Nojima fault trace at Ezaki for events 1, 4, 7, 9, 12, 13, 14, and 15 are plotted as a function of hypocentral distance. Peak amplitudes are multiplied by a factor of $(r_i/r_1)^{1/2}$, i = 1,..., 8, to correct for geometrical spreading. The straight line is the least squares fit to the eight peak amplitudes.

dimensional (2-D) profiles are somewhat different from three-dimensional (3-D) sections. However, we think it is possible to constrain the velocities on the basis of the observed *S* arrival times and the dispersive trapped waveforms. The waveguide *Q* values can be measured from the amplitude decay of trapped waves with the distance. Furthermore, the borehole logs at the Nojima fault provide some measurements of the fault width and velocities at the shallow depth [*Ito*, 1996]. Their measured width of the main shear zone (composed of the fault gouge, cataclasites, and weakly altered and deformed granodiorite rocks) at the Hirabayashi site is ~30 m at a depth around ~625 m. The measured *S* velocity for this shear zone is 1.0-2.0 km/s with the lowest velocity in the fault gouge, whereas the measured *S* velocity of the surrounding rocks is ~3.0 km/s. The borehole measurements, although valid only for the shallow part of the fault, may be used as constraints in our numerical modeling. We plan to use some more sophisticated 3-D methods such as the finite difference method to simulate the trapped waves from all recorded events for a more detailed picture of the fault zone structure.

6. Discussion and Conclusion

We recorded fault zone trapped waves with frequencies of 4-7 Hz, relatively large amplitudes, and long duration after *S* waves from Kobe aftershocks at our linear seismic arrays deployed across the Nojima fault on Awaji Island, Japan, in 1996. Such waves have been observed by *Ito and Kuwahara* [1995] and *Nishigami et al.* [1995] in their experiments on Awaji Island immediately after the Kobe earthquake.

We interpret these waves as coherent multiple reflections at the boundaries between the low-velocity fault zone and the high-velocity wall rock, when the aftershock occurred within the fault zone. We attributed this low-velocity waveguide on the Nojima fault to the dynamic rupture during the *M*7.2 earthquake of 1995. However, we did not observe significant fault zone trapped waves at the Higashiura fault located 5 km apart from the Nojima fault, suggesting the lack of a distinct low-velocity waveguide along it. In fact, the Higashiura fault did not break for at least 400 years [*Awata et al.*, 1996; *Sangawa et al.*, 1996].

The amplitude spectra of trapped waves at the Nojima fault allow us to study the attenuation of these waves as a function of station distance from the fault trace and as a function of hypocentral distance. We estimated an apparent *Q* value of ~20-30 at 4-7 Hz for the Nojima waveguide. The measured *Q* value may be affected by contamination of other phases, such as direct *S* waves [*Ben-Zion and Aki*, 1990]. However, because *S* waves decay more quickly than trapped waves, the effects of *S* waves on the *Q* value estimate are diminished as the distance increases.

To evaluate the widths and velocities of the fault zone waveguide, we simulated observed trapped waves. We obtained the best fit to observations using the waveguide parameters; the width is 30-60 m for the Nojima fault and 35 m for the Higashiura fault. The *S* velocity is 1.5-1.7 km/s and *Q*~25 for the Nojima fault. The *S* velocity is 2.5 km/s and *Q*~80 for the Higashiura fault. These model parameters are consistent with the borehole measurements at the Nojima fault [*Ito*, 1996; *Ikeda, University of Southern California*, oral communication, 1997], although valid only for the shallow part of the fault. The measured width of the main shear zone in the Hirabayashi borehole is ~30 m at a borehole depth range between 500 and 750 m, corresponding to the measured fault dip angle of 84°. The measured *S* velocity for the shear zone is 1.0-2.0 km/s but is 3.0 km/s for the surrounding rocks [*Ito*, 1996]. However, the waveguide width on the Nojima fault is only about one third of the waveguide width on the Landers fault [*Li et al.*, 1994a, b]. This may be due to different types of the Landers earthquake and the Kobe earthquake and also due to different rupture lengths and stress drops in the two earthquakes.

From the point of view of fracture mechanics, the distinct low-velocity waveguide on the Nojima and Asano faults may represent a process zone of inelastic deformation around the propagating crack tip [e.g., *Ida*, 1973; *Aki*, 1979; *Rice*, 1980; *Papageorgiou and Aki*, 1983; *Scholz et al.*, 1993; *Marone and Kilgore*, 1993]. It is reasonable that the waveguide could be softened by the dynamic rupture in the Kobe earthquake, although it more likely represents a wear zone that has accumulated over geological time. The in situ fault healing (strengthening) has been found at the Calaveras, California, fault by *Marone et al.* [1995] when they analyzed the data collected from repeating earthquakes occurring on the same fault patch [*Vidale et al.*, 1994]. Recently, repeated explosions at the Landers, California, fault showed an increase of velocities of the fault zone after the 1992 *M*7.5 earthquake [*Li et al.*, 1998]. The fault zone trapped waves recorded at the San Jacinto fault zone near Anza, California, showed the existence of a soft waveguide on the fault strand ruptured in the 1918 M6.9 earthquake but the lack of a clear waveguide on the strands which did not break recently [*Li et al.*, 1997b]. The trapped wave data taken from Nojima and Higashiura faults may also support this broken-then-healing cycle of an active fault.

We infer from the event locations (Figure 9) that the low-velocity waveguide on the northern Awaji Island extends at least 15 km along the Nojima and Asano faults and is at least 16 km deep with a southeastward dip angle of 80°-85°. However, only 9 km of surface breaks along the Nojima fault was produced by the Kobe earthquake. According to the extent of this low-velocity waveguide, we suggest that the subsurface

Figure 5a. Fault zone-parallel component of raw and low-pass-filtered (< 6 Hz) seismograms at the Ezaki array for events 10, 17, 13, 9, 1, and 14 on the Nojima and Asano faults with increasing hypocentral distances from the array. The *S* arrivals are aligned at 2.8 s (denoted by the first arrow in each plot). The second arrow denotes the duration of fault zone trapped waves. Other notations are the same as in Figure 2.

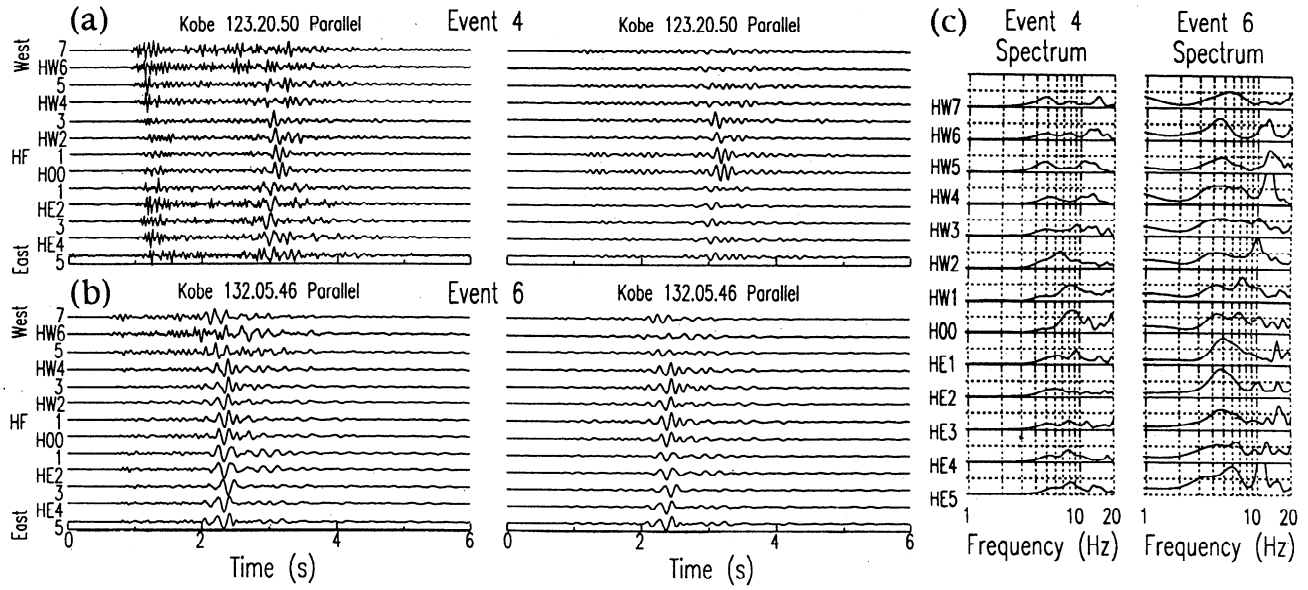

Figure 6. Fault-parallel component raw and low-pass-filtered (< 6 Hz) seismograms at the Higashiura array for (a) event 4 on the Nojima fault and (b) event 6 neither on the Nojima fault nor on the Higashiura fault. The wave trains following *S* waves are much shorter than those shown in Figure 2. (c) Normalized spectra plotted using a fixed amplitude scale of 100. Other notations are the same as in Figure 2.

rupture segment on Awaji Island is at least 15 km long. This length is longer than surface breaks but shorter than the length of the southwestern rupture plane resulted by *Wald* [1996].

Because no trapped waves were observed at the arrays deployed across the Nojima fault for aftershocks occurring on the Suma and Suwayama faults on the main island, we interpret that the Nojima fault is significantly offset from the Suma fault, although both faults were ruptured in the Kobe earthquake. Alternatively, there may be no low-velocity zone for the Suma fault, a possibility which we can not confirm because we had no arrays deployed on the main island. However, numerical investigations of trapped waves show that a fault offset of more than several fault zone widths would disrupt the waveguide [*Li and Vidale*, 1996]. At Landers, we observed that trapped waves were disrupted by a fault step-over between the northern and southern rupture segments [*Li et al.*, 1997a, b].

The above mentioned fault offset is consistent with several earlier findings. After the Kobe earthquake, the Japan Maritime Safety Agency carried out marine surveys on Akashi

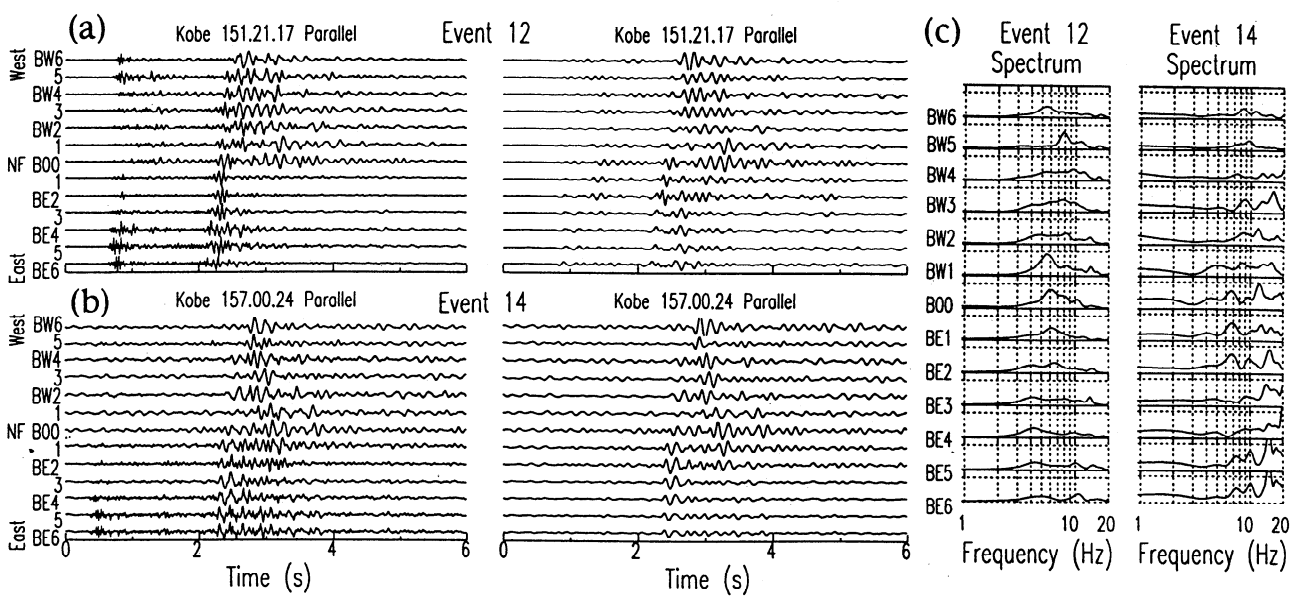

Figure 7. Fault-parallel component of raw and low-pass-filtered (< 8 Hz) seismograms at the Hirabayashi array for (a) event 12 on the Nojima fault and (b) event 14 on the Asano fault. The longest trapped wave train is shown at station B00 located right on the fault trace. (c) Normalized spectra of seismograms plotted using a fixed amplitude scale of 65 for event 12 but 35 for event 14. Peak amplitudes with 6-7 Hz appear at stations between BW1 and BE2. Other notations are the same as in Figure 2.

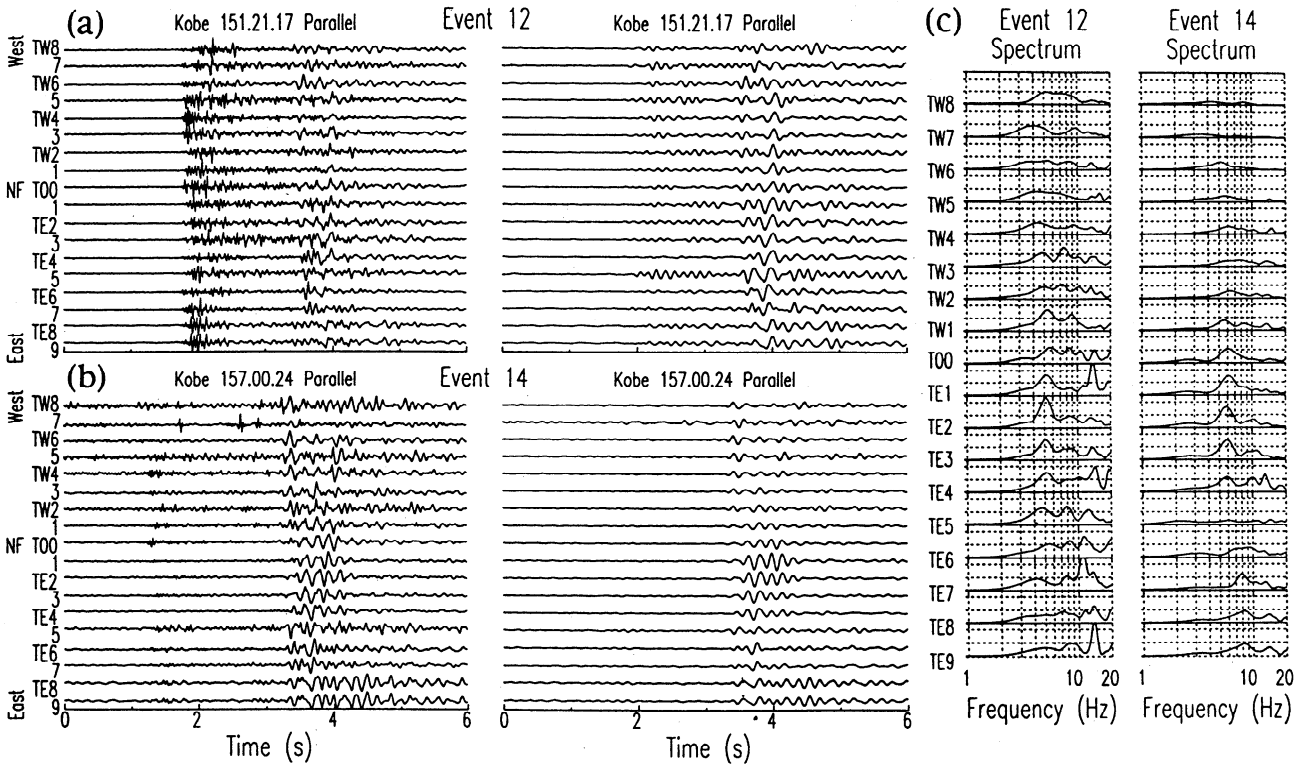

Figure 8. Fault-parallel component of raw and low-pass-filtered (< 8 Hz) seismograms at the Toshima array for (a) event 12 on the Nojima fault and (b) event 14 on the Asano fault. (c) Normalized spectra of seismograms plotted using a fixed amplitude scale of 50. Other notations are the same as in Figure 2.

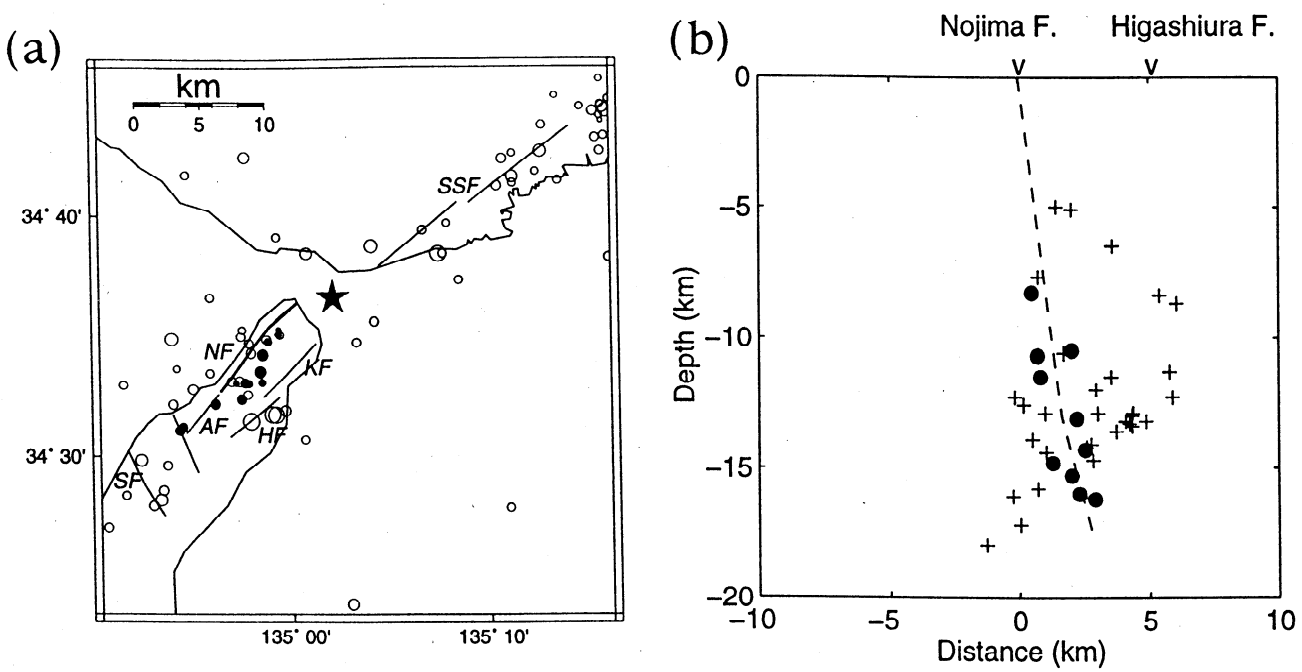

Figure 9. (a) Map showing epicenters of aftershocks occurring during the experiment. Solid circles denote the events for which we observed fault zone trapped waves, while open circles denote events without trapped waves. The star denotes the mainshock epicenter. NF, Nojima fault; SSF, Suma and Suwayama faults. Other notations are the same as in Figure 1. (b) The vertical cross section of the Nojima and Higashiura faults (surface traces indicated by v), showing locations of aftershocks occurring southwest of Akashi Strait. Solid circles denote events for which trapped waves were recorded at arrays across the Nojima fault. Crosses denote events for which no trapped waves were recorded at any array. The dashed line denotes the interpreted fault plane waveguide on the Nojima fault.

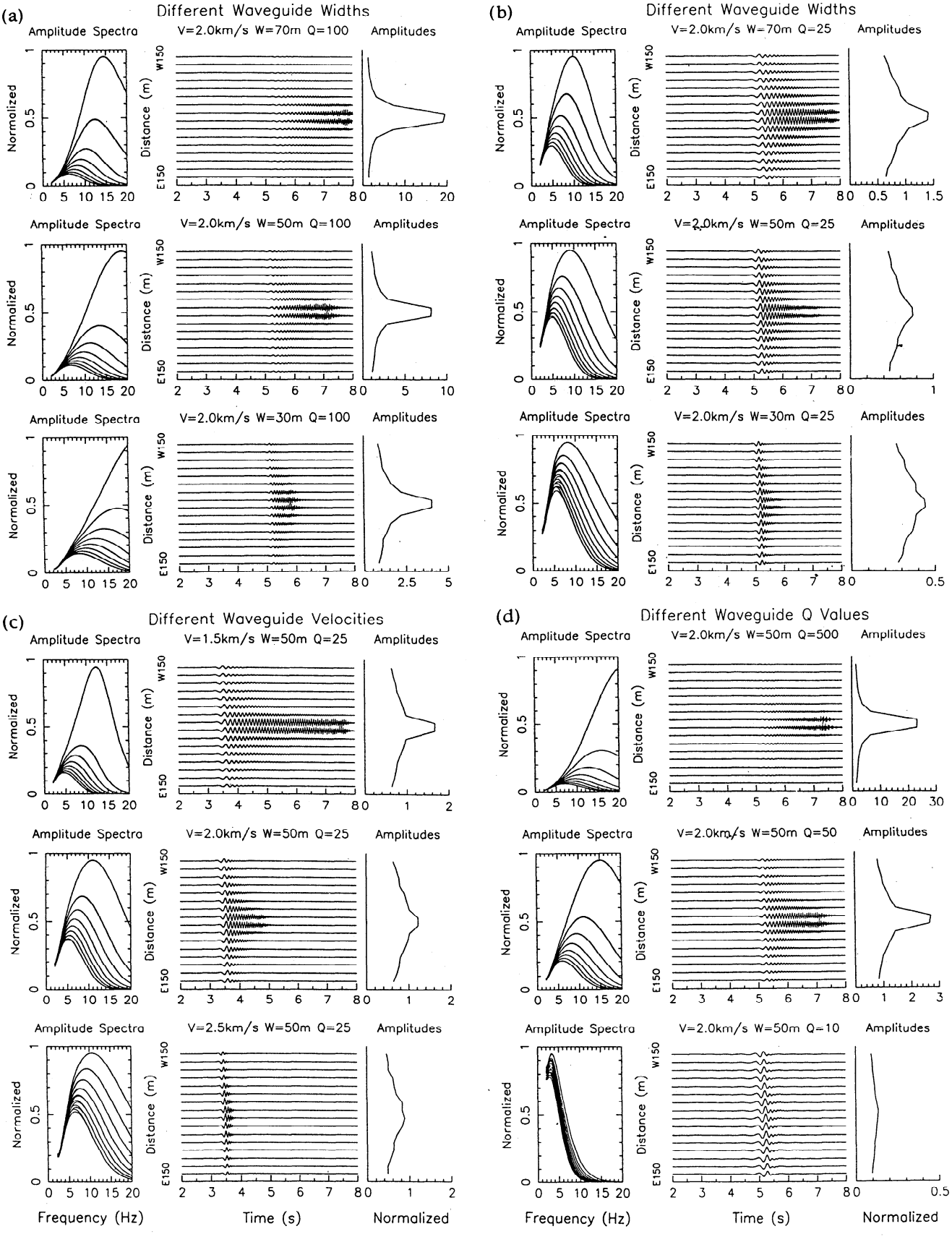

Figure 10. (a) (left) Amplitude spectra, (middle) waveforms, and (right) peak amplitudes of synthetic trapped waves for a 16-receiver array using model parameters: the waveguide S velocity of 2.0 km/s, Q value 100, and widths 70, 50, and 30 m. The receiver spacing is 20 m. A unit source is located in the middle of the waveguide, and the distance between the array and source is 15 km. The half-space has the S velocity of 3.0 km/s and Q value 100. Peak amplitudes are plotted using a fixed value in each plot. (b) Same as Figure 10a, except for the waveguide with Q value 25. (c) Same as Figure 10a, except for the waveguide with the width 50 m, Q value 100, and S velocities of 1.5, 2.0, and 2.5 km/s. The distance between the source and receiver is 10 km. (d) Same as Figure 10a, except for the waveguide with the S velocity of 2.0 km/s, width 50 m, and Q values 500, 50, and 10. The distance between the source and receiver is 15 km.

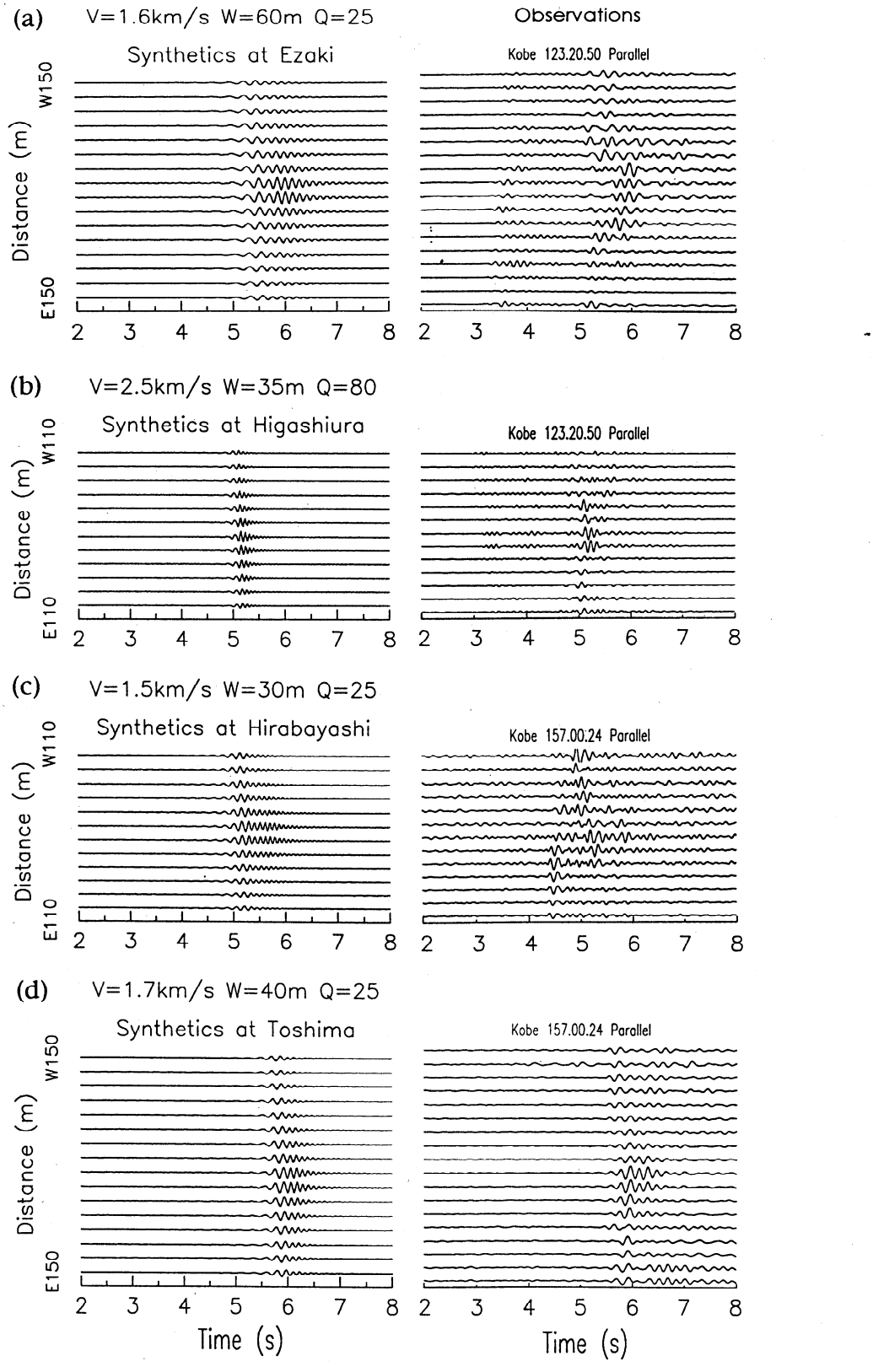

Figure 11. (left) Synthetic trapped waveforms and (right) observed seismograms at (a) the Ezaki array for event 4, (b) the Higashiura array for event 4, (c) the Hirabayashi array for event 14, and (d) the Toshima array for event 14. Seismograms are band-pass-filtered (2-8 Hz). Waveguide parameters used in computations are shown on the figure and Table 2. The receiver spacing for synthetic seismograms is 20 m. A fixed scale is used for seismograms in each plot.

Table 2. Nojima Waveguide Model Parameters

Parameters	Sites			
	Ezaki	Hirabayashi	Toshima	Higashiura
Waveguide width, m	60	30	40	35
Waveguide velocity, km/s	1.6	1.5	1.7	2.5
Waveguide Q value	25	25	25	80
Wall rock velocity, km/s	3.0	3.0	3.0	3.2
Surrounding rock Q value	100	100	100	100

Strait and found a 300-m-long offshore extension of the Nojima rupture segment [*Somerville,* 1995]. The surveys also found that the two ruptured fault segments ~7 km long were parallel to the Nojima fault but offset from it by ~5 km. Inversions of near-source ground motions, teleseismic body waveforms and geodetic displacements of the Kobe earthquake showed a complex source process with multiple subevents triggered on segmented slip planes in accordance with the distribution of the fault system in the Kobe/Awaji region. *Wald* [1996] used a 20-km-long rupture segment on Awaji Island and a 40-km-long rupture segment on the main island with an offset between them beneath the Akashi Strait. This offset caused 3-4 s rupture hesitation and might also disrupt the waveguide there. Furthermore, *Wald's* [1996] model predicts the maximum slip of 3.0 m in the shallow part (0-5 km depth) of the northern Nojima fault, where we delineated a wider low-velocity waveguide using trapped waves.

Acknowledgments. This research was supported by the National Science Foundation (grant EAR-9526330). The authors heartily thank H. Ito, Y. Kuwahara, K. Nishigami, A. Hasemi, M. Koizumi, K. Tadokoro, and S. Kwanishi for their collaborations in deployment of seismic arrays and the land owners and town officers for the permission to deploy instruments in their properties on Awaji Island. Kinya Nishigami kindly provided the catalog of local seismicity from the automatic hypocenter location system at Disaster Prevention Research Institute, Kyoto University. We are grateful to K. Shimazaki, M. Ando, K. Irikura, N. Sumitomo, R. Ikeda, and Y. Hisada for discussions on this experiment. We appreciate field assistance provided by Michael Watkins, and we thank John McRaney for his help managing this experiment. The manuscript was improved by reviews from Associate Editor Chi-Yu King, reviewer Kinya Nishigami and an anonymous reviewer. We acknowledge the support of IRIS-PASSCAL Instrument Center for the use of PASSCAL instruments.

References

Aki, K., Analysis of the seismic coda of local earthquakes as scattered waves, *J. Geophys. Res., 74,* 615-631, 1969.

Aki, K., Characterization of barriers on an earthquake fault, *J. Geophys. Res., 84,* 6,140-6,148, 1979.

Aki, K., and P. C. Richards, *Quantitative seismology,* W. H. Freeman, New York, 1980.

Awata, Y., T. Sumii, M. Yanagida, J. Begg, and R. V. Dissen, Most recent faulting on the Higashiura fault, northeast coast of the Awaji Island, central Japan (abstract), *Proc. 1996 Japan Earth Planet. Sci. Meet.,* P149, 1996.

Ben-Zion, Y., and K. Aki, Seismic radiation from an *SH* line source in a laterally heterogeneous planar fault, *Bull. Seismol. Soc. Am., 80,* 971-994, 1990.

Hamilton, J. C., K. Okumura, T. Echigo, and H. Nishida, Documentation of surface rupture at three selected sites along the Nojima fault on Awaji Island, produced by the January 17, 1995 Hyogo-Ken Nanbu (Kobe), Japan, earthquake (abstract), *Eos Trans. AGU, 76*(46), Fall Meet. Suppl., F377, 1995.

Hashimoto, M., Coseismic displacements of the Kobe earthquake of January 17, 1995, and its fault model (abstract), *Eos Trans. AGU, 76*(46), Fall Meet. Suppl., F376, 1995.

Hough, S. E., Y. Ben-Zion, and P. C. Leary, Fault-zone waves observed at the southern Joshua Tree earthquake rupture zone, *Bull. Seismol. Soc. Am., 80,* 761-767, 1994.

Huzita, K., Role of the median tectonic line in the Quaternary tectonics of the Japanese islands, *Mem. Geol. Soc. Jpn., 18,* 129-153, 1980.

Huzita, K., and T. Kazama, Geology of the Osaka-Seihokubu district, quadrangle-series (in Japanese with English abstract), scale 1:50,000, *Geol. Surv. Jpn .,* Tsukuba, 1980.

Ida, Y., The maximum acceleration of seismic ground motion, *Bull. Seismol. Soc. Am., 63,* 959-968, 1973.

Ide, S., M. Takeo, and Y. Yoshida, Source process of the 1995 Kobe earthquake: Determination of spatio-temporal slip distribution by Bayesian modeling, *Bull. Seismol. Soc. Am., 86,* 547-566, 1996.

Ito, H., Structure and physical properties of the Nojima fault, paper presented at U.S.-Japan Natural Resources, 10th Biennial Meeting, hosted by *Southern California Earthquake Center and U.S. Geol. Surv.,* Pasadena, Calif., 1996.

Ito, H., and Y. Kuwahara, Trapped waves along the Nojima fault from the aftershock of Kobe earthquake, 1995 (abstract), *Eos Trans. AGU, 76*(46), Fall Meet. Suppl., F377, 1995.

Jongmans, D., and P. E. Malin, Microearthquake *S*-wave observations from 0 to 1 km in the Varian Well at Parkfield, California, *Bull. Seismol. Soc. Am., 85,* 1805-1820, 1995.

Kanamori, H., Mode of strain release associated with major earthquakes in Japan, *Annu. Rev. Earth Planet. Sci., 1,* 213-239, 1973.

Kanamori, H., The Kobe (Hyogo-ken Nanbu), Japan, earthquake of January 16, 1995, *Seismol. Res. Lett., 66*(2), 6-10, 1995.

Kikuchi, M., The source mechanism of the Hyogoken Nanbu earthquake of January 17, 1995, *YCU (Yokohama City University) Seismol. Rep., 38,* 1995.

Leary, P. C., Y. Ben-Zion, H. Igel, and P. Mora, Modeling San Andreas fault trapped waves with a 2D analytic expression for a layered fault zone between two quarterspaces (abstract), *Eos Trans. AGU, 72*(44), Fall Meet. Suppl., F307, 1991.

Li, Y. G., and P. C. Leary, Fault zone trapped seismic waves, *Bull. Seismol. Soc. Am., 80,* 1245-1271, 1990.

Li, Y. G., and J. E. Vidale, Low-velocity fault zone guided waves: Numerical investigations of trapping efficiency, *Bull. Seismol. Soc. Am., 86,* 371-378, 1996.

Li, Y. G., P. C. Leary, K. Aki, and P. E. Malin, Seismic trapped modes in the Oroville and San Andreas fault zones, *Science, 249,* 763-766, 1990.

Li, Y. G., K. Aki, D. Adams, A. Hasemi, and W. H. K. Lee, Seismic guided waves trapped in the fault zone of the Landers, California, earthquake of 1992, *J. Geophys. Res., 99,* 11,705-11,722, 1994a.

Li, Y. G., J. E. Vidale, K. Aki, C. J. Marone, and W. H. K. Lee, Fine structure of the Landers fault zone: Segmentation and the rupture process, *Science, 256,* 367-370, 1994b.

Li, Y. G., W. L. Ellsworth, C. H. Thurber, P. E. Malin, and K. Aki, Observations of fault-zone trapped waves excited by explosions at the San Andreas fault, central California, *Bull. Seismol. Soc. Am., 87,* 210-221, 1997a.

Li, Y. G., F. L. Vernon, and K. Aki, San Jacinto fault-zone guided waves: A discrimination for recently active fault strands near Anza, California, *J. Geophys. Res., 102,* 11,689-11,701, 1997b.

Li, Y. G., J. E. Vidale, K. Aki, F. Xu, and T. Burdette, Evidence of shallow fault zone strengthening after the 1992 *M*7.5 Landers, California, earthquake, *Science, 279,* 217-219, 1998.

Malin, P. E., and M. Lou, A first observation of microearthquake F_R waves, *Eos Trans. AGU, 76*(46), Fall Meet. Suppl., F398, 1995.

Marone, C., and B. Kilgore, Scaling of the critical slip distance for seismic faulting with shear strain in fault zones, *Nature, 362,* 618-621, 1993.

Marone, C., J. E. Vidale, and W. L. Ellsworth, Fault healing inferred from time dependent variations in source properties of repeating earthquakes, *Geophys. Res. Lett., 22,* 3095-3098, 1995.

Nakamura, M., and M. Ando, Aftershock distribution of the January 17, 1995 Kobe earthquake determined by the JHD method, *Eos Trans., AGU, 76*(46), Fall Meet. Suppl., F377, 1995.

Nakata, T., and K. Yomogida, Surface fault characteristics of the 1995 Hyogoken-Namibia earthquake, *J. Nat. Disaster Sci., 16*(3), 1-10, 1995.

Nishigami, K., Y. Fujiwara, and Y. Shimada, Fault-zone trapped waves observed at the Nojima fault for aftershocks accompanying the 1995 Kobe earthquake (abstract), *Eos Trans., AGU, 76*(46), Fall Meet. Suppl., F378, 1995.

Oike, K., *Japan Earthquake Islands,* 382 pp., Asahi Press, Tokyo, 1992.

Okada, A., and Y. Ikeda, Active faults and neotectonics in Japan, *Quat. Res., 30,* 161-174, 1991.

Papageorgiou, A. S., and K. Aki, A specific offset model for the quantitative description of inhomogeneous faulting and the prediction of strong motion, I, Description of the model, *Bull. Seismol. Soc. Am.*, *73*, 693-722, 1983.

Pitarka, A., K. Irikura, and T. Kagawa, Source complexity of the January 17, 1995 Hyogoken-Nanbu earthquake determined by near-field strong motion modeling: Preliminary results, *J. Nat. Disaster.*, *16*(3), 31-37, 1995.

Research Group for Active Faults in Japan, *Active Faults in Japan: Sheet Maps and Inventories*, rev. edi., 437 pp., Univ. of Tokyo Press, Tokyo, 1991.

Rice, J. R., The mechanics of earthquake rupture, *in Physics of the Earth's Interior*, edited by A. M. Dziewonski and E. Boschi, pp. 555-649, North-Holland, Amsterdam, 1980.

Sangawa, A., Y. Awata, and Y. Sugiyama, Active fault system which caused the Keichoh Fushimi earthquake (abstract), *Proc. 1996 Japan Earth Planet. Sci. Meet.*, P149, 1996.

Scholz, C. H., N. H. Dawers, J. Z. Yu, and M. H. Anders, Fault growth and fault scaling laws: Preliminary results, *J. Geophys. Res.*, *98*(B12), 21,951-21,961, 1993.

Shimazaki, K., and T. Nakata, Time-predictable recurrence model for large earthquakes, *Geophys. Res. Lett.*, *7*, 279-282, 1980.

Somerville, P., Kobe earthquake: An Urban disaster, *Eos Trans., AGU*, *76*(6), 49-51, 1995.

Toda, S., R. S. Stein, P. A. Reasenberg, and A. Yoshida, Stress transferred by the 1995 *M*6.9 Kobe, Japan, earthquake: Validation by seismicity rate change, and implications for stress buildup on adjacent faults (abstract), *Seismol. Res. Lett.*, *68*, 324, 1997.

Usami, T., *Destructive Catalogue of Disastrous Earthquakes in Japan*, 434 pp., Univ. of Tokyo Press, Tokyo, 1987.

Vidale, J. E., W. L. Ellsworth, A. Cole, and C. Marone, Rupture variation with recurrence interval in eighteen cycles of a small earthquake, *Nature*, *368*, 624-626, 1994.

Wald, D., A preliminary dislocation model for the 1995 Kobe (Hyogo-ken Nanbu), Japan, earthquake determined from strong motion and teleseismic waveforms, *Seismol. Res. Lett.*, *66*(4), 22-28, 1995.

Wald, D., Slip history of the 1995 Kobe, Japan, earthquake determined from strong motion, teleseismic, and geodetic data, *J. Phys. Earth*, *44*, 489-503, 1996.

Yomogida, K., and T. Nakata, Relation between seismic observations and the fault complexity of the 1995 Hyogoken-Nanbu earthquake, *J. Nat. Disaster Sci.*, *16*(3), 11-19, 1995.

Yoshida, S., K. Koketsu, B. Shibazaki, T. Sagiya, T. Kato, and Y. Yoshida, Joint inversion of near- and far-field waveforms and geodetic data for the rupture process of the 1995 Kobe earthquake, *J. Phys. Earth*, *44*, 437-454, 1996.

K. Aki and Y.-G. Li, Department of Earth Sciences, University of Southern California, Los Angeles, CA 90089-0740. (e-mail: ygli@terra.usc.edu; kaki@usc.edu)

J. E. Vidale, Department of Earth and Space Sciences, University of California, Los Angeles, CA 90095-1567. (e-mail: vidale@moho.ess.ucla.edu)

M. Alvarez, Department of Geophysics, Stanford University, Stanford, CA 94305-2215, (e-mail: alvarez@passcal10.stanford.edu)

(Received June 25, 1997; revised November 11, 1997; accepted January 13, 1998.)